Defence Science Journal, Vol. 53, No. 2, April 2003, pp. 189-198

Propagation of Small Disturbance Waves in a Fluid Flow across the Junctions between Rigid and Compliant Panels

P. K. Sen and S. Hegde
Indian Institute of Technology Delhi, New Delhi – 110 016

and

P. W. Carpenter
University of Warwick, Coventry, CV 4 7AL, UK

ABSTRACT

The problem of wave propagation in a fluid flow across the junction between the rigid and the compliant panels in a channel has been studied. In vortical Tollmien-Schlichting-type waves, the jump conditions are obtained by the half-Fourier transforms defined on both the sides of the junction along with the adjoint method. The method developed is fairly generic and is applicable to similar problems. A comparison of the results obtained in the present study with those obtained from direct numerical simulations[1] shows good agreement.

Keywords: Wave propagation, fluid flow, panels, adjoint method, compliant walls, rigid-compliant panels, Tollmien-Schlichting waves, compliant panels

1. INTRODUCTION

The use of compliant walls for drag reduction, by keeping the flow laminar for large Reynolds numbers, is well studied. The evolution of two dimensional Tollmien-Schlichting (T-S) waves over alternate rigid-compliant panels through numerical simulations[2-4] was studied by the authors. It was noticed in their simulations that the propagating T-S wave exhibits a sudden change in the amplitude at the rigid-compliant wall junction. It is necessary to calculate relationship between the amplitudes on two sides of the junction. A vibrating ribbon-type transfer interface is assumed at the wall junction in the present study[6]. Once the amplitude ratios are determined at the leading and trailing edges of the compliant panel, it is possible to simulate the T-S wave and the other waves over the entire stretch of rigid and compliant panels. Simulations are carried out for a few typical cases of propagating disturbance waves.

2. ELASTIC WAVES ON PLATES AT THE JUNCTION

Before going into the details of formulation and solution of the problem, a compliant wall excitation study by Lucy[5], *et al.* has been considered. The compliant wall model used is the well-known stretched membrane model used by Carpenter and Garrad[2] in their study. The equation for this compliant wall model is given as

Received 24 October 2002

$$m\frac{\partial^2\eta}{\partial t^2}+d\frac{\partial\eta}{\partial t}+B\frac{\partial^4\eta}{\partial x^4}+K\eta=-p_w \qquad (1)$$

where η is the vertical displacement of the plate, x is in the streamwise direction, t is the time, m, d, and B are the density, damping, and flexural rigidity of the plate, respectively; K is the spring stiffness of the continuous foundation. In general, p_w is the fluid pressure acting on the plate. Here, it is equivalently zero. If the plate is driven at a frequency, β and if it is above cutoff frequency i.e, $\beta>\sqrt{K/m}$, then waves will propagate along the plate. Further, generally $d=0$ and the four fundamental solutions of Eqn (1) are:

$$e^{(i\alpha x-i\beta t)};\ \alpha=\pm\tilde{\alpha},\pm i\tilde{\alpha};\quad \tilde{\alpha}\equiv\left[(m\beta^2-K)/B\right]^{1/4} \qquad (2)$$

In Eqn (2), α is the wave speed. The above solutions correspond respectively to two travelling wave solutions, one travelling to the right and the other to the left; and two evanescent waves decaying for $x < 0$ and $x > 0$.

3. FORMULATION OF PROBLEM

A channel flow is considered here. The rigid-compliant-rigid region is formed having a compliant panel inserted as shown in Fig. 1. The compliant wall properties are applicable in the region from $x = x_1$ to $x = x_2$. The domain from $y = 0$ to $y = y_1$ corresponds to the half-width of the channel. The two junctions, at $x = x_1$ (the rigid-compliant wall interface) and at $x = x_2$ (the compliant-rigid interface), produce two different kinds of jump phenomena. Also, it is needed to look at what portion of the oncoming wave is transmitted and what portion of it gets reflected at these interfaces. The governing equation is the linearised Navier-Stokes equation, written below in vorticity form, in terms of the disturbance stream function $\psi=\psi(y,x,t)$:

$$\frac{\partial}{\partial t}\left(\nabla^2\psi\right)+\bar{u}\frac{\partial}{\partial x}\left(\nabla^2\psi\right)-\bar{u}''\frac{\partial\psi}{\partial x}-\frac{1}{R}\nabla^4\psi=0 \qquad (3)$$

Owing to periodic forcing on time, at constant temporal (circular) frequency ω, ψ may be written in the following form:

$$\psi(y,x,t)=f(y,x)\,e^{-i\omega t} \qquad (4)$$

For the sake of distinguishing the rigid and compliant sides, the function f(y, x) is defined in two halves as

$$f(y,x)=H(-x)f_-(y,x)+H(x)f_+(y,x) \qquad (5)$$

where, in Eqn (5), $H(x)$ is the Heaviside step function. Substituting Eqn (4) in Eqn (3) yields the operative differential equation for the problem.

$$-i\omega\left(\nabla^2 f\right)+\bar{u}\frac{\partial}{\partial x}\left(\nabla^2 f\right)-\bar{u}''\frac{\partial f}{\partial x}-\frac{1}{R}\nabla^4 f=0 \qquad (6)$$

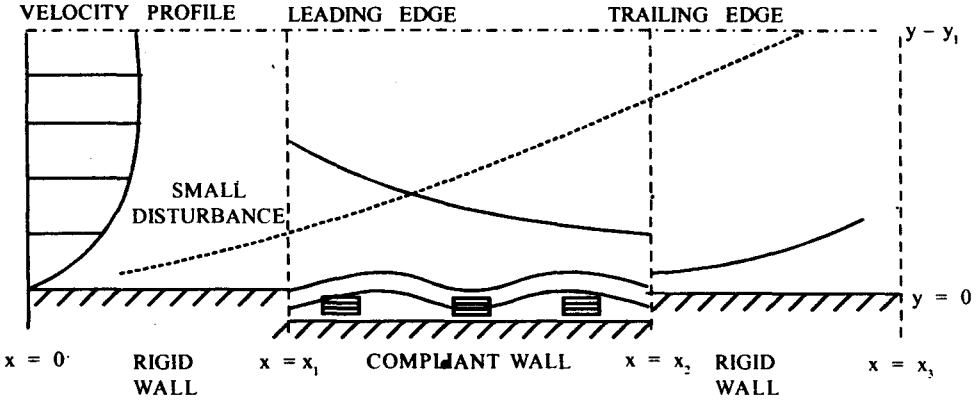

Figure 1. Rigid-compliant-rigid wall arrangement

A Fourier transform is now defined for f(y, x), in two halves, with a slit at the location of the joint, viz., at $x = 0$.

$$F_-(y,\alpha)=\int_{-\infty}^{0} f_-(y,x)e^{-i\alpha x}dx;\quad -\infty < x \le 0 \qquad (7)$$

$$F_+(y,\alpha)=\int_{0}^{+\infty} f_+(y,x)e^{-i\alpha x}dx;\quad 0 \le x < \infty \qquad (8)$$

Unlike as in a Weiner-Hopf-type of problem, f_- and f_+ are considered complete in themselves, so that the inverse transform is given separately for $-\infty < x \le 0$ and $0 \le x < \infty$. The inverse transforms are given as

$$f_- = \frac{1}{2\pi}\int_{C_a} F_-(y,x)e^{-i\alpha x}dx;\quad -\infty < x \le 0 \qquad (9)$$

$$f_+ = \frac{1}{2\pi}\int_{C_b} F_+(y,x)e^{-i\alpha x}dx;\quad 0 \le x < \infty \qquad (10)$$

where, C_a ,C_b are suitable contours enclosing the poles. The above method of representation is most convenient if the junction is to be modelled as a vibrating ribbon. If, for instance, one is dealing with just a pair of waves, viz., the rigid T-S mode for $-\infty < x \le 0$ and the compliant T-S mode for $0 \le x < \infty$, then: (i) the ribbon is created by the incident wave from the rigid side; and (ii) the compliant T-S mode $x \ge 0$ tunes in from the vibrating ribbon.

An attempt has been made to give an essential model of the vibrating ribbon. The two fringes on either side of the ribbon merge into the upstream and downstream side waves, respectively. It now remains to see at a so-called essential form or elemental form for the ribbon function. Due to rapid change in x at around $x = 0$, or the ribbon location, $\nabla^2\psi$ is essentially $\left(\frac{\partial^2\psi}{\partial x^2}\right)_{x=0}$.

This suggests the form for the ribbon function ϕ as

$$\phi = \Omega e^{-i\omega t} \qquad (11)$$

where

$$\Omega \approx \left(\frac{\partial^2 f}{\partial x^2}\right)_{x=0}$$

Now, the Fourier transform of Eqn (6) is taken separately for the domains $-\infty < x \le 0$ and $0 \le x < \infty$. For both sets of transforms, one needs to know the value of the function f(y, x) at $x = 0$. For both halves, this is given as $\nabla^2 f_-(y, x=0)=\Omega$ and $\nabla^2 f_+(y, x=0)=\Omega$. Both halves of the Fourier transformed Eqn (6), therefore, reduce to an Orr-Sommerfeld like equation with a forcing term given in terms of ϕ. The equations are as follows:

$$L(\alpha)F_- = +\Omega\bar{u} \qquad (12)$$

$$L(\alpha)F_+ = -\Omega\bar{u} \qquad (13)$$

where, in Eqns (12) and (13), the operator $L(\alpha)$ is the Orr-Sommerfeld operator. The expanded form of this operator is given as

$$L(\alpha)F = i(\alpha\bar{u}-\omega)(F''-\alpha^2F) - i\alpha\bar{u}''F - \frac{1}{R}(F''''-2\alpha^2F''+\alpha^4F) \qquad (14)$$

Now, let the rigid side be considered, i.e., $-\infty < x \le 0$, with boundary conditions applicable to the rigid side applied to F_-. Let the eigenvalue corresponding to the rigid side be α_r, In which case, in the neighbourhood of values close to α_r, Eqn (12) may be expanded as follows:

$$L(\alpha_r)F_- + (\alpha-\alpha_r)L_2(\alpha_r)F_- = +\Omega\bar{u} \qquad (15)$$

Similarly, corresponding to the compliant side, i.e., for $0 \le x < \infty$, and with appropriate boundary conditions for the compliant side applied to F_+, and remembering that the eigenvalue for the compliant side is given by α_c, one obtains:

$$L(\alpha_c)F_+ + (\alpha - \alpha_c)L_2(\alpha_c)F_+ = -\Omega\bar{u} \tag{16}$$

The operator $L_2(\alpha)$ in Eqns (15) and (16) is defined as

$$L_2(\alpha)F = i\left[\bar{u}F'' - \bar{u}''F - 3\alpha^2\bar{u}F + 2\omega\alpha F\right] - \frac{1}{R}\left[-4\alpha F'' + 4\alpha^3 F\right] \tag{17}$$

It has been noted that substituting Eqn (11) for ϕ in Eqns (15) and (16) results in

$$L(\alpha_r)F_- + (\alpha - \alpha_r)L_2(\alpha_r)F_- = +\bar{u}C \tag{18}$$

$$L(\alpha_r)F_+ + (\alpha - \alpha_r)L_2(\alpha_r)F_+ = -\bar{u}C \tag{19}$$

where, the constant C is defined as $C \equiv \Omega(y)$. In other words, essential content of Ω is a constant.

4. CALCULATION OF JUMP IN AMPLITUDE

According to the method of solution based on adjoints, the jump in the amplitude of the disturbance wave may be generically defined by a factor λ, as follows. Consider, for example, the rigid side disturbance wave is defined as

$$\phi_r(y)e^{i(\alpha_r x - \omega t)} = \lambda_r\bar{\phi}_r(y)e^{i(\alpha_r x - \omega t)} \tag{20}$$

where overline (–) over ϕ will generically denote a suitably normalised ϕ, eg $\phi = 1 + i0$ at $y = 1$. Thereafter, the magnitude of λ will generically define the magnitude of the jump. Using this convention, and using methods based on adjoint theory, it is noted that

$$\lambda_r = \frac{C\int_0^1 \theta_r\bar{u}dy}{\int_0^1 \left[L_2(\alpha_r)\bar{\phi}_r\right]\theta_r dy} \tag{21}$$

where, in Eqn (21) and subsequently, θ_r will (generically) imply the adjoint eigenfunction to ϕ_r. Actually Eqn (21) depicts the creation of the ribbon. The magnitude of the rigid side wave may be defined as $\lambda = 1$, whereupon, one obtains the value of C as

$$C = \frac{\int_0^1 \left[L_2(\alpha_r)\bar{\phi}_r\right]\theta_r dy}{\int_0^1 \theta_r\bar{u}dy} \tag{22}$$

Similarly, using Eqn (21), one may determine the magnitudes of the jumps λ_c on the compliant side as follows:

$$\lambda_c = \frac{C\int_0^1 \theta_c\bar{u}dy}{\int_0^1 L_2(\alpha_c)\,\bar{\phi}_c\theta_c dy} \tag{23}$$

where, in Eqns (20) to (23), the subscripts r and c denote quantities on the rigid side and the compliant side, respectively. But on the compliant side, the T-S wave may show up in combination with other modes. To determine the jump corresponding to each individual mode, one needs to run the programme with appropriate α_c.

5. OTHER EIGENMODES

Once the amplitude of the T-S wave λ_c on the compliant side for a given case is known, it is possible to determine the amplitudes for other eigenmodes on the compliant side as well. For this, the boundary conditions available at the two ends of the compliant panel were utilised. It was noted that at the leading edge, the wall displacement $\eta = 0$ and by assuming hinged joint at $x = 0$, one obtains the second condition as $\eta'' = 0$. Similarly, these same conditions are satisfied at $x = x_2$, the trailing edge also. On the compliant side, along with the T-S mode (α_2), one needs to consider other eigenmodes like the vorticular mode (α_2), long wave (α_3) and evanescent modes (α_4 and α_5) also. The vorticular wave is like the T-S wave but originates at the trailing edge and is an upstream travelling wave. The other mode is a long wave with a smaller wave number. Apart from these three modes, two local evanescent modes in the close vicinity of the edges are also noticed. The

combined amplitude of the compliant wall motion at the two ends of the compliant panel is calculated by adding up the individual contributions of all the relevant modes. This gives rise to four relations with four unknown amplitudes as follows:

$$e^{-i\alpha_2 L}a_2 + a_3 + a_4 + 0a_5 = -a_1 \quad (24)$$

$$a_2 + a_3 e^{-i\alpha_3 L} + a_4 + 0a_5 = -a_1 e^{-\alpha_1 L} \quad (25)$$

$$a_x^2 e^{-i\alpha_2 L}a_2 + \alpha_3^2 a_3 + \alpha_4^2 a_4 + 0a_5 = -\alpha_1^2 a_1 \quad (26)$$

$$\alpha_2^2 a_2 + \alpha_3^2 e^{-i\alpha_3 L}a_3 + 0a_4 + \alpha_5^2 a_5 = -\alpha_1^2 a_1 e^{-i\alpha_1 L} \quad (27)$$

where, in Eqns (24) to (27) a_1, a_2, a_3, a_4 and a_5 are the amplitudes of the component waves, viz., T-S wave, vorticular wave, long wave, leading edge evanescent mode and trailing edge evanescent mode, respectively. The amplitudes are computed by solving the above system of Eqns (24) to (27) using Gaussian elimination.

6. RESULTS & DISCUSSION

The formulation is verified by running the computer program for different cases. There is a very good agreement between the present results and the numerical simulations carried out by Davies and Carpenter[1]. Firstly, the simulation below cutoff frequency is investigated. The simulations above cutoff frequency are carried out in detail as it can point to important information about the stabilising aspects of the compliant surfaces. The Reynolds number is taken as R = 12000 for all the cases. Again, the wall parameter values are taken as in Davies and Carpenter[1]: In this case and in the subsequent cases, the (nondimensional) wall parameters used are: m, d, B, T, and K which denote the

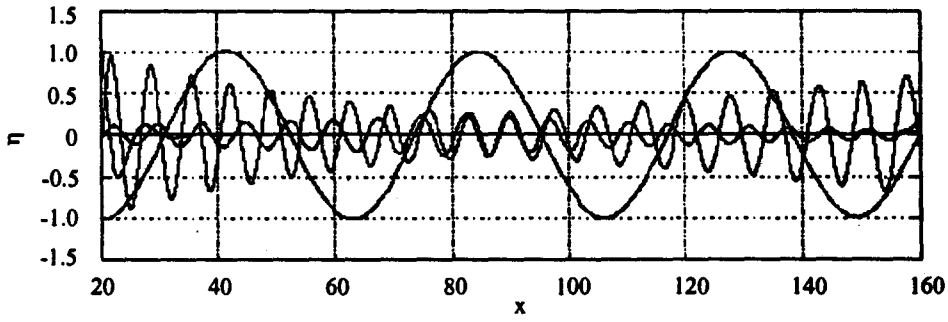

(a)

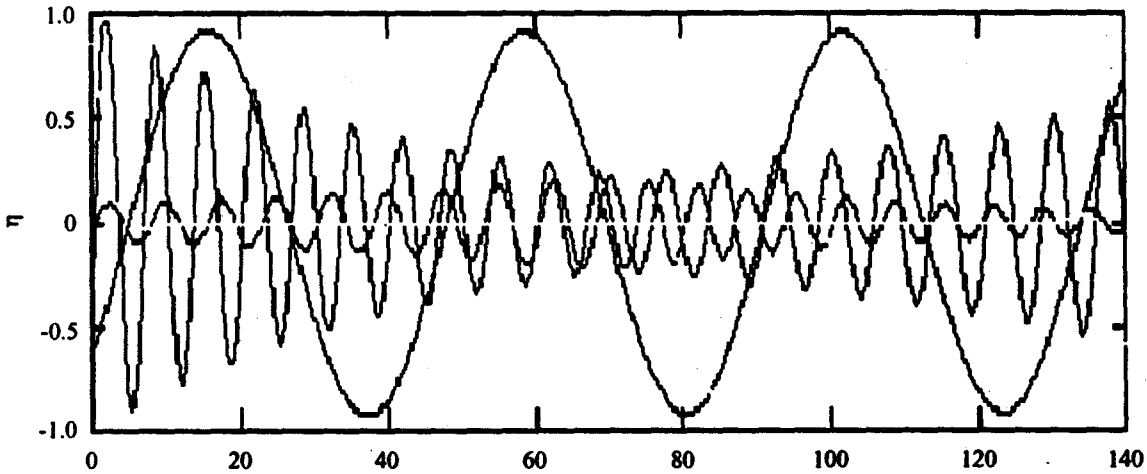

(b)

Figure 2. Compliant wall eigenmodes

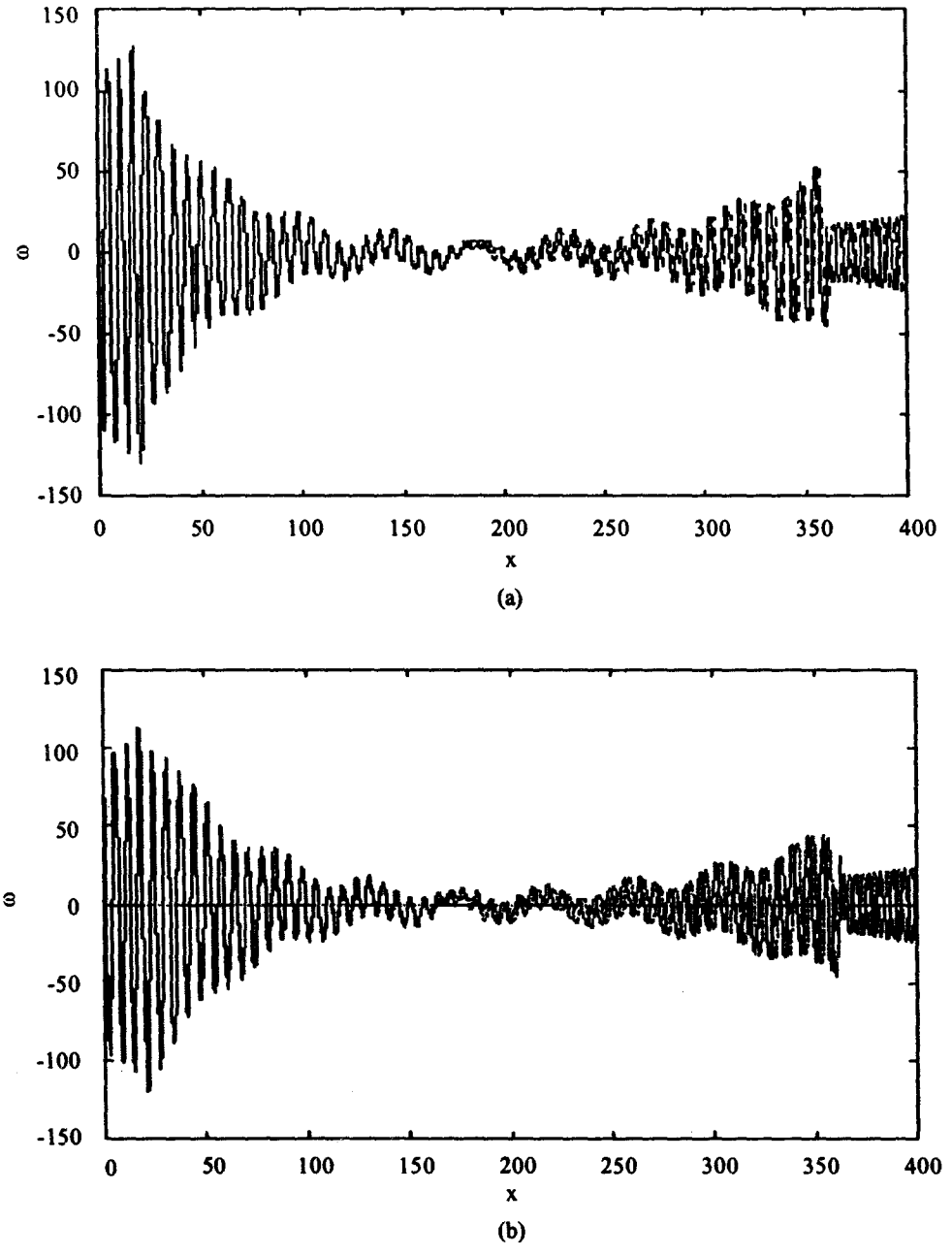

Figure 3. Compliant wall vorticity plots: (a) present results (b) corresponding results from Davies and Carpenter[1]. Nondimensional length of panel = 340 and junctions are located at x = 40, and 360.

density, damping coefficient, flexural rigidity, streamwise tension per unit length, and spring stiffness per unit area, respectively.

6.1 T-S Wave below Cutoff Frequency

For this case the wall parameters are taken as $m = 0.33333$, $T = 0$, $d = 0$, $B = 1.92 \times 10^7$, $K = 4B$. The nondimensional frequency is $\beta = 0.24$, and, from the present calculations, the eigenvalues for the rigid side and for the compliant side are respectively given as follows:

$$\alpha_r = 1.0317 - 0.0093i;$$

$$\alpha_c = 0.9395 + 0.0109i$$

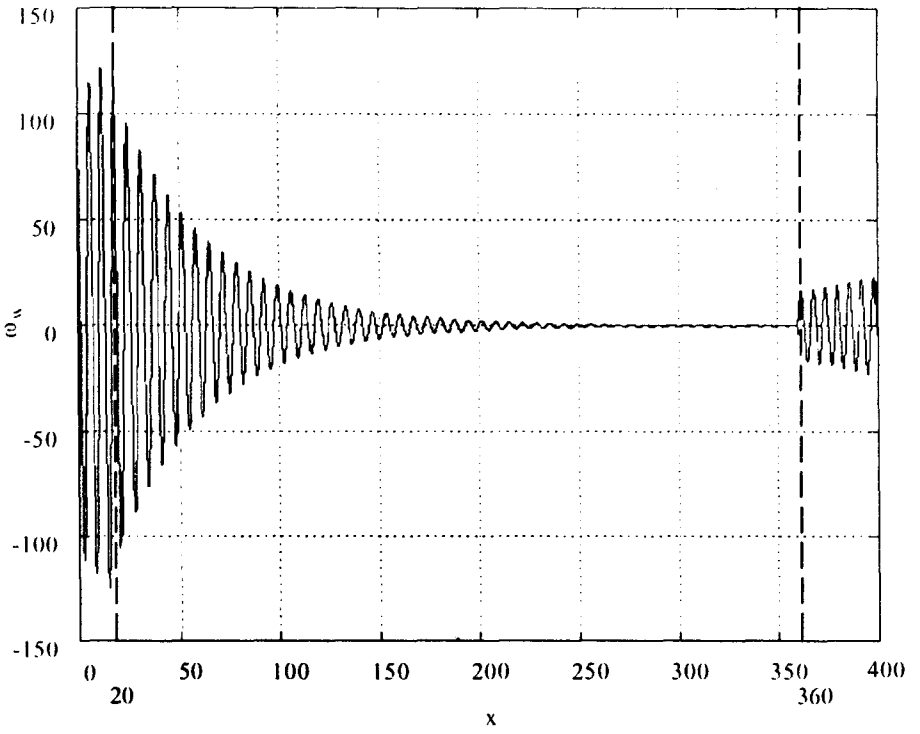

Figure 4. T-S wave component in Fig. 3(a)

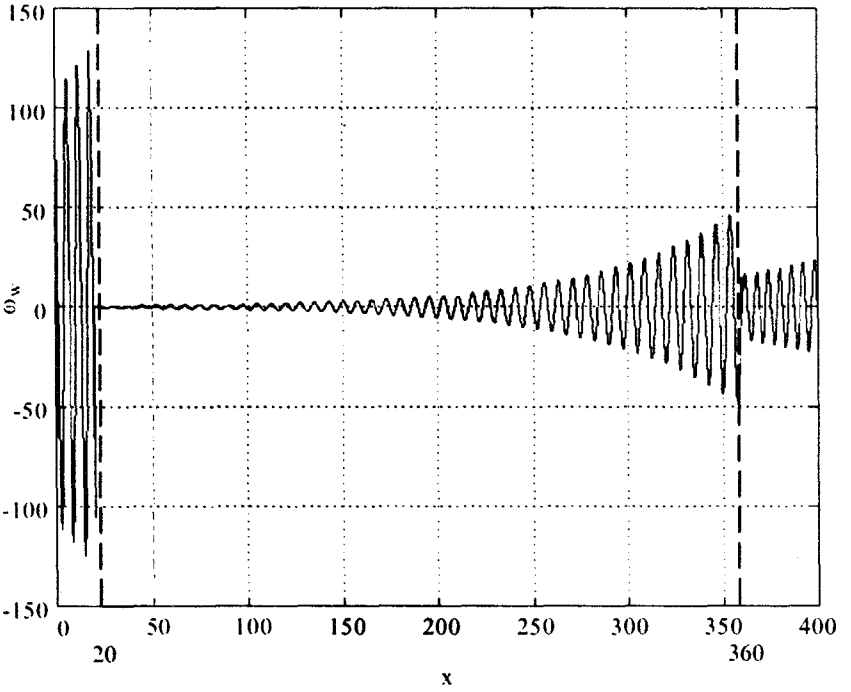

Figure 5. Vortical wave component in Fig. 3(a)

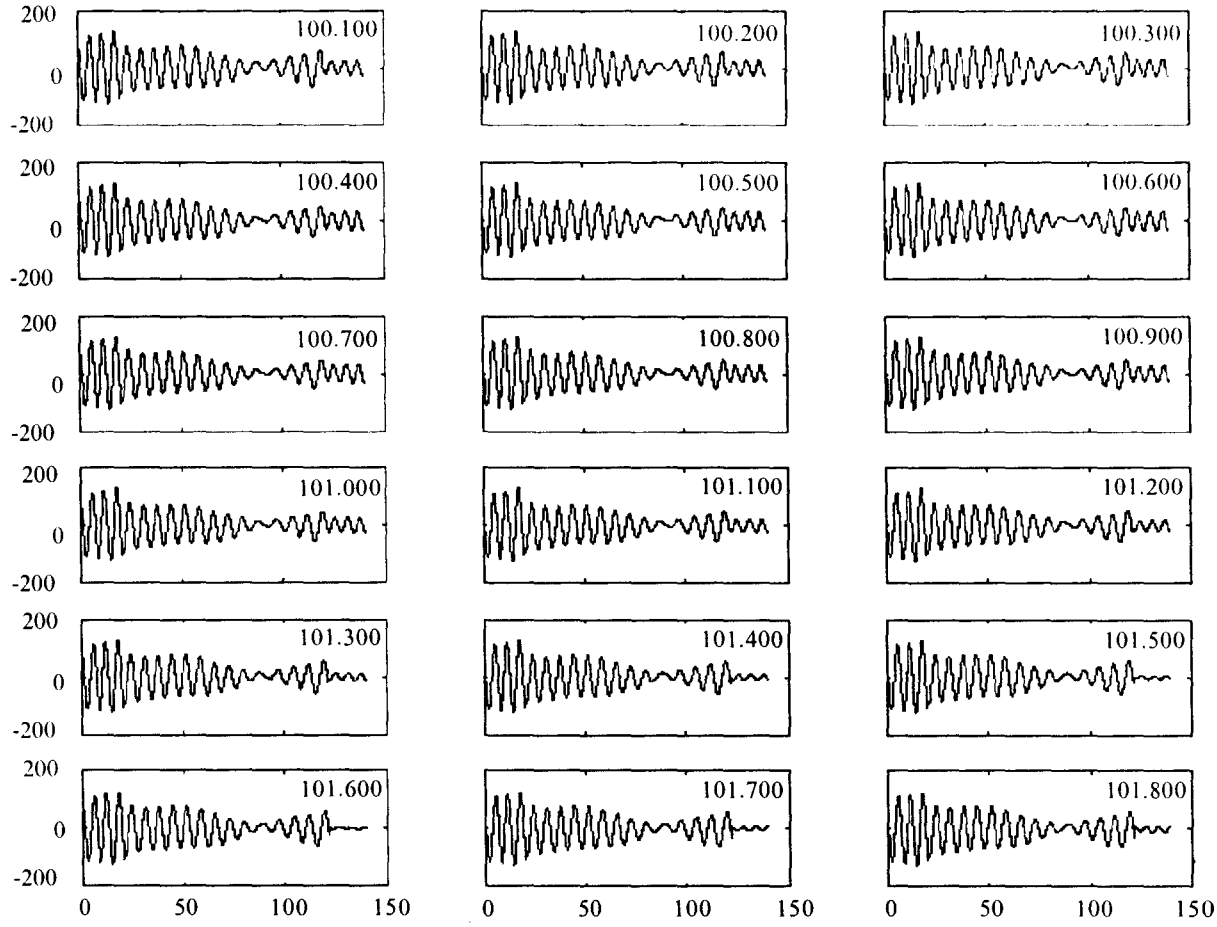

Figure 6. Compliant wall vorticity plots with small incremental length changes. The numbers on the top-right corner indicate the length of the compliant panel.

6.2 T-S Wave above Cutoff Frequency

For this case, the wall parameters are taken as $m = 0.33333$, $T = 0$, $d = 0$, $K = 1.92 \times 10^7$, $B = 4K$. The three eigenvalues for T-S mode, vorticular mode and longwave mode are calculated respectively as

$$\alpha_{ts} = 0.920795 + 0.02125i$$

$$\alpha_{vor} = -0.833156 + 0.01380i$$

$$\alpha_{l\omega} = -0.145876 + 0.00018i$$

As can be seen from the simulation results shown in Figs 2 and 3, there is a good agreement between the results obtained and those published by Davies and Carpenter[1]. An important thing, is to choose an appropriate initial phase of the wave that matches best with the similar simulations in Davies and Carpenter[1].

The individual modes on the compliant side are shown in Fig. 2. The dominant among these seem to be T-S mode and vorticular mode. The residual part of the T-S wave is transmitted across the trailing edge.

The case of a longer panel is shown in Fig. 3, wherein the wall vorticity plots for a rigid-compliant-rigid region are depicted. A clear jump was noticed in the leading edge junction and another similar but opposite kind of jump at the trailing edge. The two component waves, T-S wave and vortical wave are shown in Figs 4 and 5, respectively. These figures indicate the logic used in the calculation of the jump on the downstream rigid side. Here, the contribution is mainly from the vortical wave as the strength of the T-S wave is insignificant. This point can be observed in Figs 4 and 5.

7. EFFECT OF PANEL LENGTH ON WAVE SYSTEMS

It was mentioned that the technique developed is generic to a class of fluid flow problems. In case of numerical simulations any change in geometry of the problem requires re-running of the whole simulation. However, in the present approach, the eigensolutions obtained once in the beginning are reused, even some parameters like the length of the domain, are modified. This feature is demonstrated by changing the length of the panel in steps of small increments. The compliant wall vorticity plots for some of such steps are shown in Fig. 6. The numbers on the top-right corner indicate the length of the compliant panel. Each of these cases correspond to a different simulation in direct numerical simulation. In similar manner, the phase angles can also be altered to give different patterns of the propagating waves. Those among such patterns, which match very well with the simulation results of Davies and Carpenter[1] are used in the earlier comparisons.

8. CONCLUSIONS

A comparison of the results obtained from the present study[6] with that from the direct numerical simulations of Davies and Carpenter[1] are presented. The agreement in results validates the vibrating ribbon model for the junction and also the solution methodology based on the adjoint. The present method is very convenient in comparison to the direct numerical simulations. The present approach, being a very generic in nature, can be used as a tool for transition prediction and control. Further, this approach has a great potential for engineering applications involving the use of compliant surfaces.

REFERENCES

1. Davies, C. & Carpenter, P. W. *J. Fluid Mech.*, 1997, **335**, 361-92.

2. Carpenter, P.W. & Garrad, P.J. *J. Fluid Mech.*, 1985, **155**, 465-10.

3. Sen, P.K. & Arora D.S. *J. Fluid Mech.*, 1988, **197**, 201-40.

4. Carpenter, P.W. & Garrad P.J. *J. Fluid Mech.*, 1986, **170**, 199-32.

5. Lucy, A.D.; Sen P.K. & Carpenter, P.W. Wall excitation on a flexible surface in the presence of a uniform mean flow. *In* Proceedings of the 5th ASME International Symposium on Fluid-structure Interactions, Aeroelasticity, Flow-induced Vibrations and Noise (Accepted for publication).

6. Hegde, S. Study of small disturbance waves across alternate rigid and compliant panels with analytical jump conditions at the junctions. PhD Thesis. Applied Mechanics Dept, IIT Delhi. 2002.

Contributors

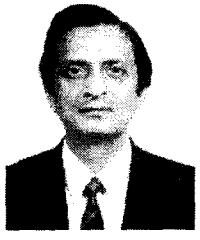

Prof PK Sen is in the Dept of Applied Mechanics at the Indian Institute of Technology Delhi. His main research interests are: Theoretical fluid mechanics, especially in hydrodynamic stability, compliant surfaces, turbulence, etc.

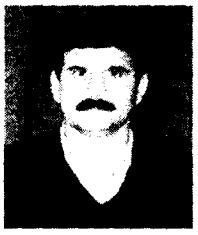

Dr S Hegde is in the Dept of Applied Mechanics at the IIT Delhi. His areas of research include: Hydrodynamic stability, computational fluid dynamics, etc.

Prof PW Carpenter is currently the Head, Civil and Mechanical Engineering Divisions at the Warwick University, UK. He is well known to the research community in the areas of hydrodynamic stability, compliant surfaces, drag reduction, turbulences, etc.